

PRELIMINARY RESULTS OF THE NEA FHR BENCHMARK PHASE I-A AND I-B (FUEL ELEMENT 2-D BENCHMARK)

**B. Petrovic^{1*}, K. Ramey¹, I. Hill², E. Losa³, M. Elsawi⁴, Z. Wu⁵, C. Lu⁵, J. Gonzalez⁶,
D. Novog⁶, G. Chee⁷, K. Huff⁷, M. Margulis⁸, N. Read⁸ and E. Shwageraus⁸**

¹Georgia Institute of Technology
Atlanta, GA, USA

²OECD/Nuclear Energy Agency (OECD/NEA)
Paris, France

³Research Centre Rez
Husinec-Řež, Czech Republic

⁴Pacific Northwest National Laboratory (PNNL)
Richland, WA, USA

⁵Virginia Commonwealth University
Richmond, VA, USA

⁶McMaster University
Hamilton, ON, Canada

⁷University of Illinois at Urbana-Champaign
Champaign, IL, USA

⁸University of Cambridge
Cambridge, UK

bojan.petrovic@gatech.edu, kmramey@gatech.edu, Ian.HILL@oecd-nea.org,
Evzen.Losa@cvrez.cz, mohamed.elsawi@pnnl.gov, zwu@vcu.edu, luc4@vcu.edu,
gonzaj10@mcmaster.ca, novog@mcmaster.ca, gchee2@illinois.edu, kdhuff@illinois.edu,
mm2353@cam.ac.uk, nr438@cam.ac.uk, es607@cam.ac.uk

dx.doi.org/10.13182/M&C21-33746

ABSTRACT

Under the auspices on OECD-NEA, a benchmark has been initiated to assess state of the art modelling and simulation capabilities for Fluoride salt-cooled High-temperature Reactors (FHRs) with TRISO fuel embedded in fuel plates (“planks”) of hexagonal fuel elements. Benchmark phases I-A and I-B involve reactor physics analysis of a representative fuel element, without and with depletion. Several configurations are considered (e.g., unrodded and rodded configuration, presence of burnable absorbers, variable enrichment). Parameters

* Corresponding author

compared include multiplication factor, reactivity coefficients, flux distribution, neutron spectrum and isotopic composition change with burnup. Seven organizations from four countries are taking part in this blind-benchmark exercise, using Monte Carlo and deterministic methods. Given the complex combination of materials and geometry, the FHR benchmark is expected to be challenging, particularly for deterministic codes. As the nuclear data libraries underpinning both deterministic and Monte Carlo methods have had limited testing for FHR systems, and molten salt systems in general, the benchmark aims to provide feedback to both the nuclear data community as well as molten salt reactor designers with regards to the variance of results with different nuclear data sources. This paper reports on the current results submitted and provides comparisons and analysis. Overall, the observed agreement is satisfactory, although notable differences are identified in specific cases, suggesting need for further in-depth analysis of those cases.

KEYWORDS: molten salt reactor (MSR), fluoride salt-cooled high-temperature reactor (FHR), TRISO, double heterogeneity, reactor physics benchmark

1. INTRODUCTION

1.1. Motivation for the FHR Benchmark

Molten salt cooled reactors offer two attractive features: high operating temperature (and high efficiency) at low (near-atmospheric) operating pressure. OECD Nuclear Energy Agency (NEA) countries collectively expressed their need to assess capabilities of existing modelling and simulation tools to analyze molten salt reactor (MSR) systems, given the novelty of the materials and geometry. One particular variant of the MSR design is the Fluoride salt-cooled High-temperature Reactor (FHR).

FHRs use molten fluoride salt as coolant, while their fuel is in TRISO form, either embedded in fuel plates (“planks”) of hexagonal fuel elements (fuel assemblies), or in circulating pebbles; this paper focuses on a benchmark of the former reactor type [1,2], developed by Oak Ridge National Laboratory (ORNL) and also known as the Advanced High Temperature Reactor (AHTR). AHTR thermal power is 3,400 MWt, and its core is composed of 252 hexagonal fuel elements, as depicted in Fig. 1. A closer look at and description of the hexagonal fuel element can be found later in Fig. 3 shown in Section 1.2.

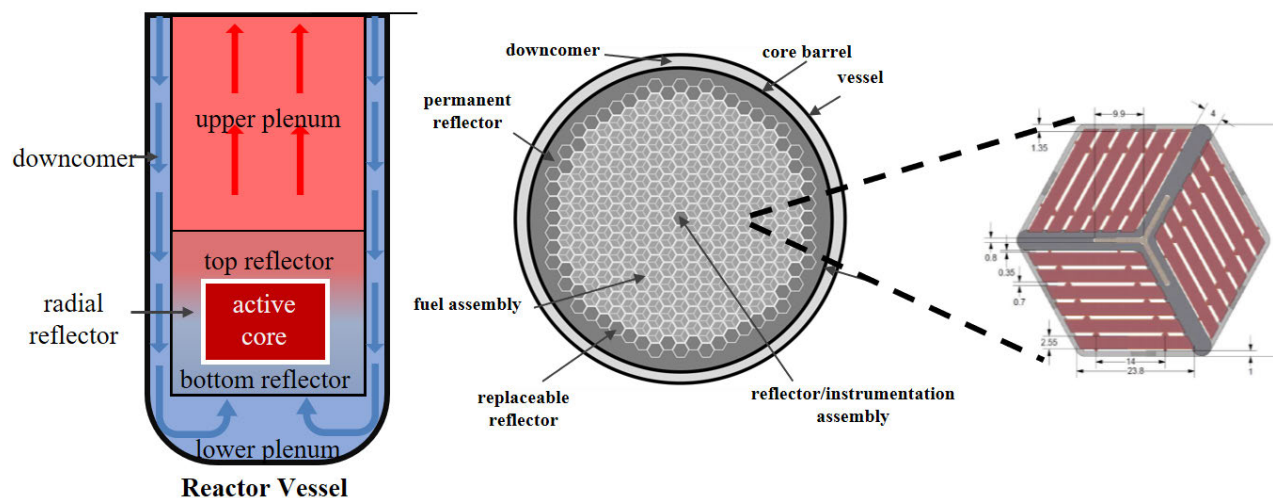


Figure 1. AHTR configuration: reactor (left), core (middle) and hexagonal fuel element (right) [1]

The geometrically complex design of fuel elements combined with double heterogeneity makes accurate FHR reactor physics simulations challenging [3,4], pointing to a need to assess accuracy of such analyses. Preliminary cross-comparison of fuel element simulation at beginning of cycle (BOC, without depletion) using Serpent [5], SCALE [6] and MCNP [7] provided good agreement for a limited number of cases considered [8]. Findings presented in [8] may be summarized as follows. The multiplication factors obtained with the three codes were within +/-300 pcm; the differences are likely at least partly attributable to different cross section libraries used. Flux distributions, compared over 3 broad energy groups (with energy cutoff at 3 eV and 0.1 MeV) exhibited good agreement, as visualized in Fig. 2. However, it also identified several areas requiring further investigation. Based on insights obtained in this preliminary analysis, an FHR Benchmark with an extended set of exercises has been developed [9]. The cross-comparison of results is conducted under the auspices of the OECD-NEA.

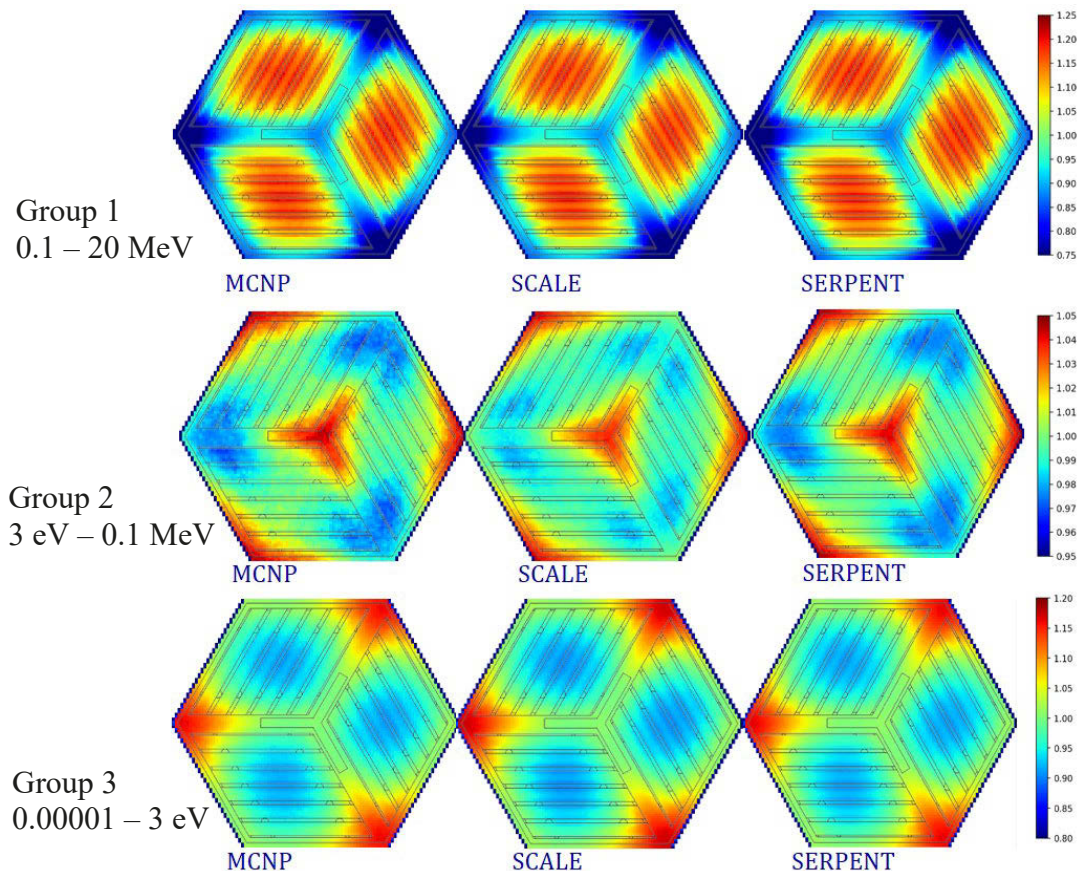


Figure 2. Comparison of neutron flux distribution over FHR fuel element, obtained by 3 codes, visualized in 3 broad energy groups with energy cutoff at 3 eV and 0.1 MeV [8]

1.2. FHR Benchmark Definition, Scope and Phases

The objective of the presented effort is to identify applicability of methods and codes, evaluating both their accuracy and practicality, and to assess the current state of the art of FHR simulations. A phased blind (or semi-blind) benchmark approach has been selected. A representative FHR hexagonal fuel element design (Figure 3) with 9 wt% fuel enrichment, no burnable poison (BP), and control rods (CR) out is taken as the base case. The following nine cases are to be analyzed:

- CASE 1: Reference case at hot full power (HFP)
- CASE 2H: Reference case at hot zero power (HZIP)
- CASE 2C: Reference case at cold zero power (CZP)
- CASE 3: CR inserted, otherwise same as CASE 1.
- CASE 4: Discrete europa BP used, otherwise same as CASE 1.
- CASE 4R: Discrete europa BP, and CR inserted, otherwise same as CASE 1.
- CASE 5: Integral (dispersed) europa BP, otherwise same as CASE 1.
- CASE 6: Twice increased HM loading (4 to 8 layers of TRISO).
- CASE 7: Fuel enrichment increased to 19.75 wt%, otherwise same as CASE 1.

The benchmark is envisioned in several phases, from fuel element analysis to multi-physics full 3D core analysis, starting with Phase I, Fuel element (2D/3D with depletion), with the following sub-phases:

- Phase I-A – “2D” (pseudo-2D) model, steady state (no depletion)
- Phase I-B – 2D model depletion
- Phase I-C – 3D model depletion

No depletion results are denoted by adding letter A to the case number (e.g., CASE 1A), while the depletion results are denoted by adding letter B (e.g., CASE 1B).

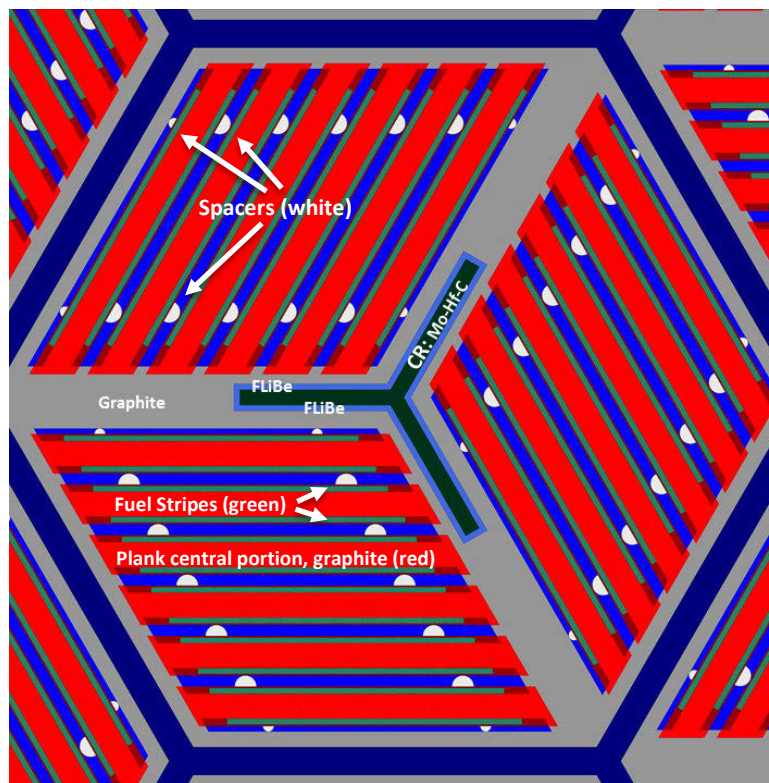


Figure 3. FHR hexagonal fuel element with fuel “planks” (shown with CR inserted)

This paper describes the currently performed Phase I-A and Phase I-B. Reactor physics parameters to be calculated and reported include: multiplication factor, reactivity coefficients, fission distribution, flux distribution, neutron spectrum, spectral indices, and isotopic composition for both fresh fuel and at selected burnups over the prescribed fuel depletion.

1.3. Benchmark Participants

Seven organizations from four countries are participating in this benchmark. The list of participants with codes employed and nuclear data libraries used is presented in Table I.

Table I. Benchmark participants.

ID	Organization	Method	Code	Library	Energy structure
CVREZ	Research Centre Rez, Czech Republic	MC	Serpent 2 [5]	ENDF/B-VII.0	CE
GT	Georgia Institute of Technology, USA	MC	Serpent 2	ENDF/B-VII.0	CE
PNNL	Pacific Northwest Nat'l Lab (PNNL), USA	MC	Serpent 2	ENDF/B-VII.0	CE
VCU	Virginia Commonwealth University, USA	MC	Serpent 2	ENDF/B-VII.0	CE
MAC	McMaster University, Canada	MC	OpenMC [10]	ENDF/B-VII.1	CE
UIUC	University of Illinois at Urbana-Champaign, USA	MC	OpenMC	ENDF/B-VII.1	CE
CAM	University of Cambridge, UK	DET	WIMS [11]	JEFF-3.1.2	MG 172

MC = Monte Carlo; DET = deterministic; CE = continuous energy; MG = multigroup

2. RESULTS

Participants were asked to submit results without knowledge of other submissions, making the initial iteration 'blind'. Thus obtained results were reviewed, and while the agreement was rather good in large majority of cases and comparisons, several outliers with larger differences were identified. These outliers were mostly traced to differences in interpretation of the benchmark specifications, and in some cases to input error. Due to the complexity of the geometry and materials distribution, it was not surprising that specifications were ambiguous in some instances. Some inaccuracies in modeling details were detected as well and corrected. This resulted in a limited number of updates; however, no "tweaking" of the models or methods was performed for the purpose of obtaining better agreement. Out of potentially 63 sets of results (nine cases and seven participants), only one case has been excluded, due to specific issues likely related to nuclear data, as explained later.

Six key reactor physics parameters (multiplication factor, reactivity coefficients, fission density distribution, neutron flux spectrum and distribution, and fuel isotopics) were compared, either as integral values or as 2D distributions, for several depletion steps. This produced significant amount of quantitative data to assess the models and perform cross-verification providing insight into potential causes of the differences. Due to space limitations, only selected results are presented here. Additional cross-comparisons are expected to be presented in a focused and detailed benchmark report.

2.1. Multiplication Factor

Comparison of the multiplication factor, k , for all cases analyzed is presented in Fig. 4 and Table II. Results have been anonymized, i.e., each participant's results are represented by a specific symbol or line color, but the legend that would be used to identify individual participants is not provided in any figure. A similar anonymization has been followed throughout the whole paper. For all cases the standard deviation is in the range of 78-141 pcm, which is very good given that the benchmark was semi-blind. Considering the complicated nature of this non-water moderated multiplying system with double heterogeneity, and recognizing that 3 different codes were used employing continuous energy and multigroup data coming from 3 different nuclear libraries, the overall agreement is noteworthy. Note that the result for one case

(Case 3, participant 6) has been removed, since the large difference in the multiplication factor was traced to the difference in molybdenum cross sections in the nuclear data library used. [12]

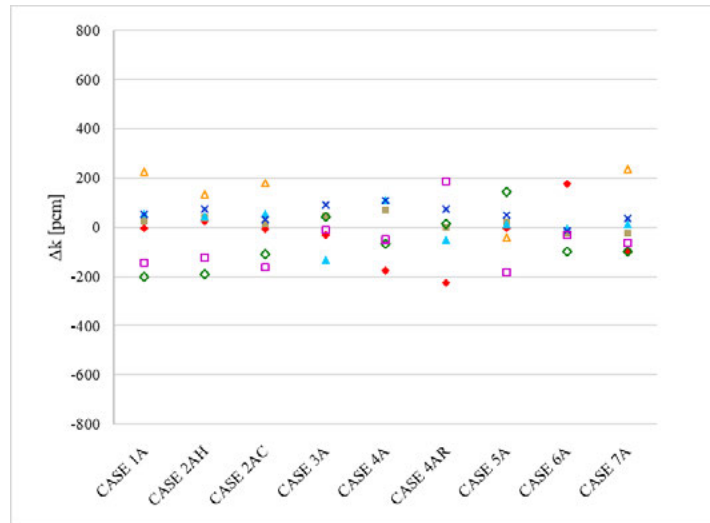


Figure 4. Graphic comparison of obtained multiplication factors (k) for nine cases considered

Table II. Quantitative comparison of obtained multiplication factors (k) for nine cases considered.

CASE	1	2	3	4	5	6	7	Average	$\sigma_k(\text{pcm})$
CASE 1	1.39559	1.39530	1.39590	1.39587	1.39333	1.39762	1.39389	1.39536	141
CASE 2H	1.40557	1.40540	1.40561	1.40590	1.40328	1.40650	1.40395	1.40517	114
CASE 2C	1.42065	1.42044	1.42107	1.42084	1.41944	1.42232	1.41891	1.42052	111
CASE 3	1.03205	1.03127	1.03029	1.03251	1.03200	See [10]	1.03147	1.03160	78
CASE 4	1.09886	1.09638	1.09927	1.09922	1.09748	n/a	1.09766	1.09814	116
CASE 4R	0.83969	0.83745	0.83922	0.84045	0.83982	n/a	0.84158	0.83970	137
CASE 5	0.80041	0.80016	0.80032	0.80068	0.80163	0.79975	0.79837	0.80019	99
CASE 6	1.26301	1.26502	1.26324	1.26313	1.26228	n/a	1.26294	1.26327	92
CASE 7	1.50567	1.50496	1.50604	1.50625	1.50493	1.50828	1.50526	1.50591	116
Max 1 σ	0.00003	0.00004	0.00015	0.00023	0.00008	n/a	0.00011		78-141

NOTE: Each column represents results by one participant. Results are provided in a randomized order.

2.2. Reactivity Temperature Coefficients

Reactivity temperature coefficients were obtained by changing separately the temperature of fuel, coolant (FLiBe) and graphite, by $\pm 50\text{K}$, and estimating by $\Delta\rho/\Delta T$ the value of the coefficient at the midpoint temperature, corresponding to the baseline temperature for that material in each case. The associated statistical uncertainties were propagated. Results are shown in Fig. 5 for the fuel (left figure), FLiBe (center figure) and graphite (right figure) coefficient, respectively. Results have again been anonymized. With exception of several isolated points, the results agree fairly well, among themselves and with the expected values. For the fuel temperature coefficient (left figure), values for the reference Case 1A are in the -2.2 to -3.1 pcm/K range, with all values within ± 0.5 pcm/K from the average. A similar and acceptable spread is observed in all Cases. With a significant hardening of spectrum in Cases 4AR (discrete BP and CR inserted),

5A (dispersed BP) and 6A (twice reduced carbon-to-HM ratio), the fuel temperature coefficient becomes more negative. For the FLiBe coolant temperature coefficient, previous studies reported values around zero, and similar values are also observed in the middle figure. More negative values are again obtained for Cases 4AR, 5A and 6A, and the spread of values in each case is again approximately ± 0.5 pcm/K from the average. Finally, graphite temperature coefficients are shown in the right figure. In most Cases the agreement is good and the spread is similar as for fuel and FLiBe. However, several values differ from the rest more than expected; specifically, the blue triangle for Cases 3A, 4A and 4AR, the red diamond in Case 3A, and the square in Case 4A. These cases will be further examined aiming to identify the source of the differences. Since there are multiple carbonaceous structures (some carbon and some graphite with corresponding $S(\alpha, \beta)$ matrices) in the complicated geometrical model, the most likely culprit is inconsistencies in the modelling of these regions.

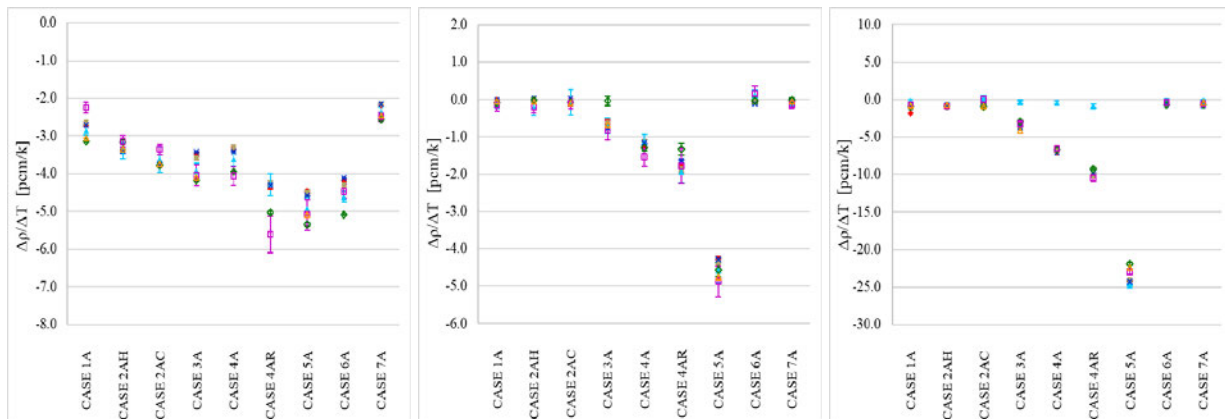


Figure 5. Reactivity Temperature Coefficients: fuel (left), FLiBe coolant (middle), graphite (right)

2.3. Fission density distribution

Each fuel stripe with TRISO particles is divided longitudinally into five sections for the purpose of obtaining the fission density distribution (Fig. 6). There are two fuel stripes per fuel plank, and eighteen fuel planks per fuel element (Fig. 1 and Fig. 3), which defines 180 distinct regions for fuel density distribution. This is a similar granularity to a PWR 17x17 fuel element with 264 fuel pins. However, due to 120-degree periodic symmetry in the reflected single-element simulation, we obtain only 60 different values. In the ensuing figures, fission density values are plotted against the position index, which in each case goes from 1 to 60, even though the actual locations are not linearly arranged. Moreover, to enable compact presentation, we combine all 9 cases into a sequence of 540 values (9 times 60). The objective is to visually depict the range of differences rather than to point to specific locations. Fig. 7 presents the differences of all Monte Carlo results for all cases against the average values, shown as the ratio to the average. For the first seven cases (index 1 through 420), the minimum and maximum ratio of all values is 0.990 and 1.013, i.e., practically within $\pm 1\%$. The differences are somewhat higher for the last two cases (Case 6A and 7A), with the minimum and maximum ratio being 0.985 and 1.018, but the large majority is still within $\pm 1\%$, and all are well within $\pm 2\%$, quite impressive overall agreement. The associated statistical uncertainties on Monte Carlo simulations range—depending on the participant—from 0.0003 to 0.002 (i.e., 0.03% to 0.2%). Fission density distribution obtained by deterministic calculations exhibits slightly higher differences, but the minimum and maximum difference to the average remains within $\pm 3\%$ for all cases analyzed (five out of nine defined Cases). This agreement is at least as impressive considering all the differences between continuous-energy Monte Carlo simulations and a multigroup deterministic calculation.

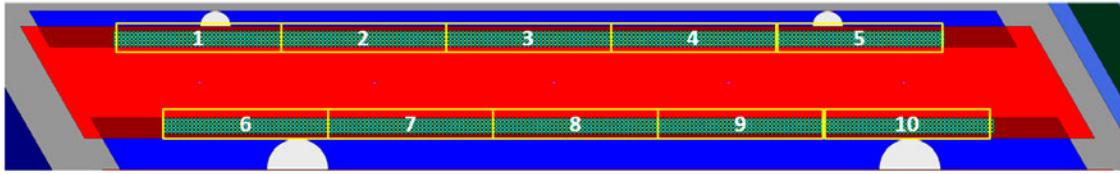


Figure 6. Definition of 10 fission density regions in each fuel plank

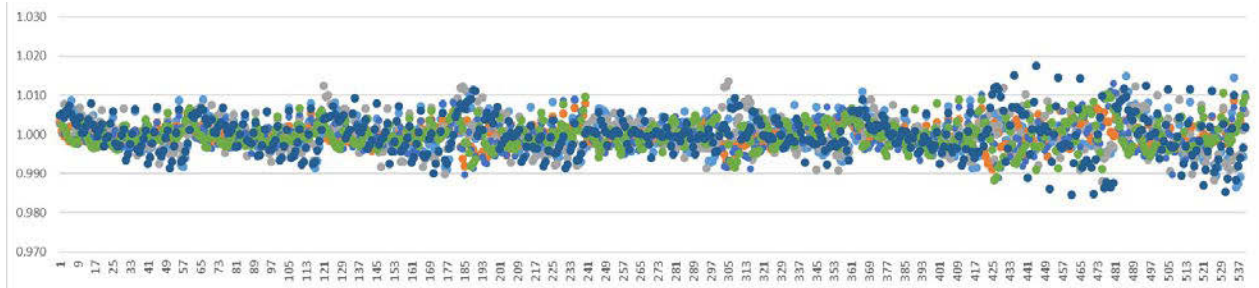


Figure 7. Ratio of individual-to-average fission density obtained for the 9 benchmark Cases by Monte Carlo simulations from 6 participants for 60 fission density regions in each case

2.4. Neutron Spectra

Benchmark specifications requested multigroup fluxes, preferably in the SCALE 252-group structure; this energy structure was used for tallying by all Monte Carlo codes. For deterministic calculations, the multigroup library itself dictated the energy structure. Multigroup fluxes per unit lethargy represent spectrum; additionally, normalization was performed for easier comparison. However, instead of the usual normalization to the unit integral, spectra were normalized to the maximum value in each case. Anonymized spectra for Case 1A are compared in Fig. 8. Statistical error bars are not show since they would been indiscernible. A good agreement is observed with spectral features corresponding to the materials present in the problem definition. A similar agreement is observed in other Cases.

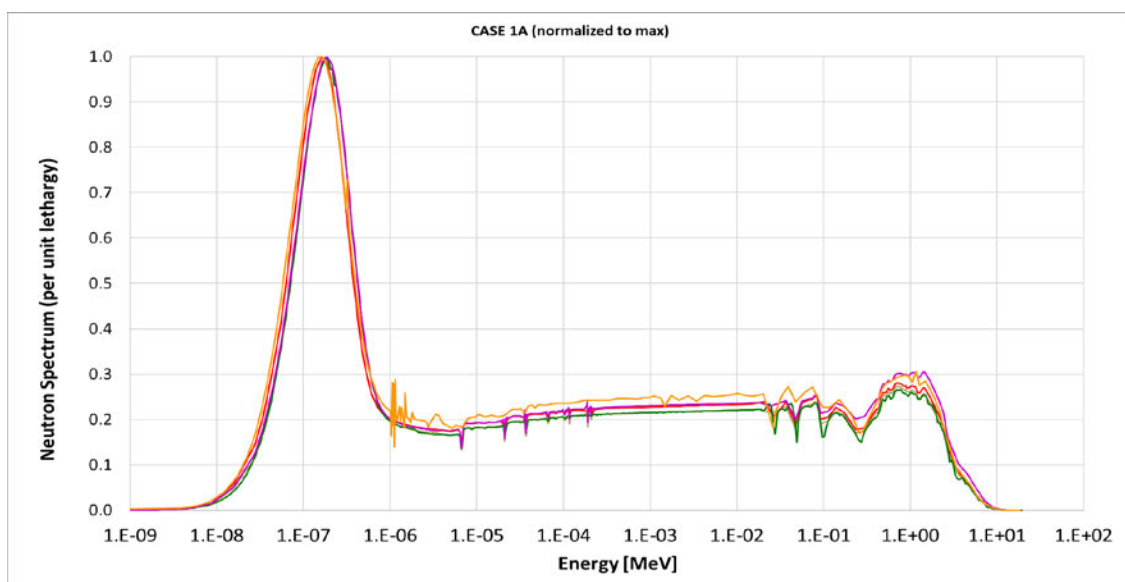


Figure 8. Comparison of normalized neutron spectra for Case 1A

2.4. Depletion

Cases 1, 4 and 7 were depleted using prescribed depletion steps. Since Phase I-B of the benchmark focuses on depletion, these results are denoted as Cases 1B, 4B and 7B, as opposed to Cases 1A, 4A and 7A denoting zero-burnup analyses. Cases 1B and 4B were depleted to 70 GWd/tU, while Case 7B deploying higher enriched fuel (19.75 wt% vs 9 wt%) was depleted to 160 GWd/tU. Comparison of important parameters including criticality, fission distribution, flux distribution, and neutron spectrum (similar to zero-burnup cases in Phase I-A) was performed at selected burnups. Due to the space limitations, only the comparison of multiplication factors is presented here. A detailed report is being prepared that will include much more extensive comparisons.

Figure 9 compares multiplication factors for the reference Case 1B. Statistical uncertainty, not shown in the Figure, was less than 50 pcm in all cases. The agreement is generally good; however, there is a slight divergence with burnup. Main suspects for this divergence are the recoverable energy per fission and possibly different models available in different codes (e.g., depletion with and without critical spectrum). This will be further examined to identify the culprit.

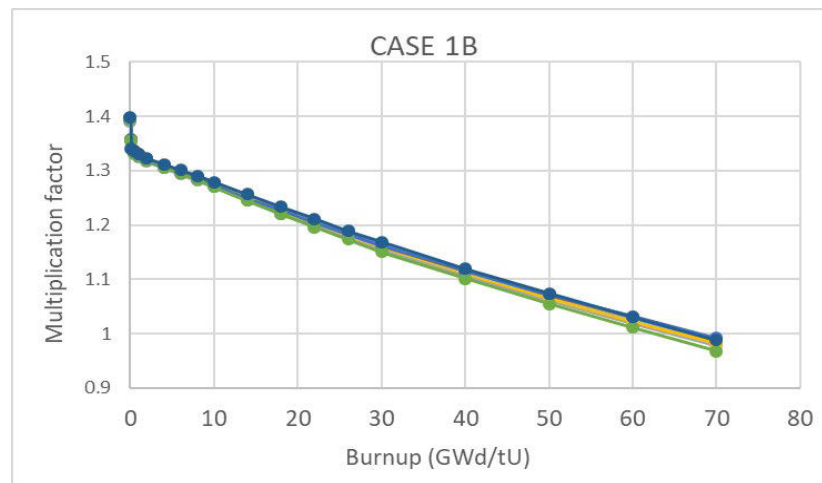


Figure 9. Comparison of multiplication factor vs. burnup for Case 1B

2.5. Isotopics and additional results

Additional results have been obtained for all nine cases in Phase I-A and for the three selected cases in Phase I-B. They have been compared, but because of the space limitations could not have been presented and discussed in this paper. They include: (a) spectral indices; (b) flux distribution; (c) isotopics. The agreement is generally good, as with the presented results, but in some specific cases further evaluation may be warranted.

3. CONCLUSIONS

There is commercial interest in developing and deploying FHRs, but applicable reactor physics experiments that may be used for validation of codes are scarce. Therefore, a numerical benchmark has been established to enable cross-verification of reactor physics codes considered for simulation of FHRs. The first two phases, Phase I-A (no depletion) and Phase I-B (with depletion) focus on analysis of a single reflected hexagonal

fuel element. A blind/semi-blind benchmark is being performed with participation of 7 organizations from 4 countries. Results and cross-comparisons presented in this paper indicate satisfactory agreement in most cases, in particular considering that FHR fuel elements include a challenging complex geometry and double heterogeneity. Larger differences initially observed in a limited number of cases were investigated and in most cases their origins were identified. This benchmark offers a valuable cross-verification opportunity to commercial efforts aimed at designing and licensing FHRs; it also provides a challenging problem that may be used to test the capabilities of modern reactor physics codes and validity of modeling methodologies. This benchmark will allow the community to assess the impact of new models and nuclear data libraries on FHR systems, for a variety of neutronics parameters. Extension of the benchmark to full 3D core analysis with depletion (Phase II) and feedback (Phase III) is foreseen.

ACKNOWLEDGMENTS

The presented work is part of a broader effort to benchmark FHR modeling and simulations involving seven team members from four countries. The benchmark is performed under the auspices of OECD NEA.

REFERENCES

1. D.E. Holcomb, D. Ilas, V.K. Varma, A.T. Cisneros, R.P. Kelly, J.C. Gehin, "Core and Refueling Design Studies for the Advanced High Temperature Reactor," *ORNL/TM-2011/365*, Oak Ridge National Laboratory (2011).
2. V.K. Varma, D.E. Holcomb, F.J. Peretz, E.C. Bradley, D. Ilas, A.L. Qualls, N.M. Zaharia, "AHTR Mechanical, Structural, and Neutronic Preconceptual Design," *ORNL/TM-2012/320*, Oak Ridge National Laboratory (2011).
3. K. Ramey, B. Petrovic, "Monte Carlo Modeling and Simulations of AHTR Fuel Assembly to Support V&V of FHR Core Physics Methods," *Annals of Nuclear Energy*, **118**, pp. 272-282 (2018).
4. F. Rahnema, B. Petrovic, P. Singh, P. Burke, H. Noorani, X. Sun, G. Yoder, P. Tsvetkov, J. Zhang, D. Zhang, D. Ilas, "The Challenges in Modeling and Simulation of Fluoride-Salt-Cooled High-Temperature Reactors," *White Paper CRMP-2017-9-001*, Georgia Institute of Technology (2017).
5. J. Leppänen, M. Pusa, T. Viitanen, V. Valtavirta, T. Kaltiainenaho, "The Serpent Monte Carlo Code: Status, Development, and Applications," *Ann. of Nucl. Energy*, **82**, pp. 142-150 (2015).
6. "SCALE 6.2.1: A Comprehensive Modeling and Simulation Suite for Nuclear Safety Analysis and Design; Includes ORIGEN and AMPX," *ORNL/TM-2005/39*, Version 6.2.1, Oak Ridge National Laboratory, Oak Ridge, TN (2016).
7. "MCNP—A General Monte Carlo N-Particle Transport Code," Version 6.1, LA-UR-03-1987, Los Alamos National Laboratory, Los Alamos, N.M. (2013).
8. B. Petrovic, T. Flaspöehler, K. Ramey, "Benchmarking FHR Core Physics Simulations: 2D Fuel Assembly Model," *Proc. 12th Intl. Conf. on Nuclear Option in Countries with Small and Medium Electricity Grids*, Zadar, Croatia, June 3-6, 2018 (2018).
9. NEA (Prepared by B. Petrovic, K. Ramey and I. Hill), "Benchmark Specifications for the Fluoride-salt High-temperature Reactor (FHR) Reactor Physics Calculations, Phase I-A and I-B: Fuel Element 2D Benchmark," Nuclear Science, OECD Publishing, Paris, France (2021).
10. P. K. Romano, N. E. Horelik, B. R. Herman, A. G. Nelson, B. Forget, and K. Smith, "OpenMC: A State-of-the-Art Monte Carlo Code for Research and Development," *Ann. Nucl. Energy*, **82**, 90–97 (2015).
11. The ANSWERS Software Service, "WIMS A Modular Scheme for Neutronics Calculations - User Guide for Version 10," ANSWERS/WIMS/REPORT/014 (2015).
12. K. Ramey, M. Margulis, N. Read, E. Shwageraus, and B. Petrovic, "Impact of Molybdenum Cross Sections on FHR Analysis," submitted to *Nuclear Engineering and Technology*.